Isolation of *Neisseria gonorrhoeae* Mutants That Show Enhanced Trafficking across Polarized T84 Epithelial Monolayers

SYLVIA HOPPER,[1]* J. SCOTT WILBUR,[1] BRANDI L. VASQUEZ,[1] JASON LARSON,[1]
SUSAN CLARY,[1] IAN J. MEHR,[2]† H. S. SEIFERT,[2] AND MAGDALENE SO[1]

*Department of Molecular Microbiology and Immunology, Oregon Health Sciences University,
Portland, Oregon 97201-3098,[1] and Department of Microbiology-Immunology,
Northwestern University Medical School, Chicago, Illinois 60611[2]*

Initiation of a gonococcal infection involves attachment of *Neisseria gonorrhoeae* to the plasma membrane of an epithelial cell in the mucosal epithelium and its internalization, transepithelial trafficking, and exocytosis from the basal membrane. Piliation and expression of certain Opa proteins and the immunoglobulin A1 protease influence the transcytosis process. We are interested in identifying other genetic determinants of *N. gonorrhoeae* that play a role in transcellular trafficking. Using polarized T84 monolayers as a model epithelial barrier, we have assayed an *N. gonorrhoeae* FA1090 minitransposon (mTn) mutant bank for isolates that traverse the monolayer more quickly than the isogenic wild-type (WT) strain. From an initial screen, we isolated four mutants, defining three genetic loci, that traverse monolayers significantly more quickly than their WT parent strain. These mutants adhere to and invade cells normally and do not affect the integrity of the monolayer barrier. Backcrosses of the mutations into the WT FA1090 strain yielded mutants with a similar fast-trafficking phenotype. In two mutants, the mTns had inserted 370 bp apart into the same locus, which we have named *fit*, for fast intracellular trafficker. Backcrosses of one of these mutants into the MS11A genetic background also yielded a fast-trafficking mutant. The *fit* locus contains two overlapping open reading frames, *fitA* and *fitB*, whose deduced amino acid sequences have predicted molecular weights of 8.6 and 15.3, respectively. Neither protein contains a signal sequence. FitA has a potential helix-turn-helix motif, while the deduced sequence of FitB offers no clues to its function. *fitA* or *fitB* homologues are present in the genomes of *Pseudomonas syringae* and *Rhizobium meliloti*, but not *Neisseria meningitidis*. Replication of the MS11A *fitA* mutant in A431 and T84 cells is significantly accelerated compared to that of the isogenic WT strain. In contrast, growth of this mutant in liquid media is normal. Taken together, these results strongly suggest that traversal of *N. gonorrhoeae* across an epithelial barrier is linked to intracellular bacterial growth.

Neisseria gonorrhoeae (i.e., the gonococcus [GC]) gains access to the human body primarily at the mucosal epithelia of the urogenital tract. In most cases, GC causes a simple, self-limiting local infection (gonorrhea). However, it also has the ability to disseminate to other sites, among them the joints (to cause gonococcal arthritis) and the fallopian tubes (to cause salpingitis, tubal blockage, and infertility). Infection can also lead to the establishment of a carrier state; the population of apparently healthy individuals harboring infectious bacteria is considered a major factor in the transmission of gonococcal disease.

Interactions of GC with the epithelial cell surface have been studied extensively using organ and cell culture systems. These studies demonstrate that upon contact, the bacteria initially form a loose association with the epithelial cell, adhering as microcolonies at the tips of clusters of elongated microvilli and on the plasma membrane (19, 33). At later times of infection, the bacterial aggregates disperse and GC are seen tightly adhered as a monolayer on the host cell surface (34). At this stage, the bacterial and the host cell plasma membranes are closely juxtaposed (15).

Numerous bacterial cell surface components play a role in GC-host cell interactions. Type IV pili promote initial attachment of GC to the epithelial cell (8, 24, 25, 53; J. G. Cannon, M. S. Cohen, S. F. Isbey, T. L. Snodgrass, A. Wallace, J. A. F. Dempsey, M. Apicella, and D. Zhou, Abstr. 10th Int. Pathog. *Neisseria* Conf., p. 11–12, 1996); its receptor has been identified as CD46 (membrane cofactor protein [23]). Pilus-mediated adhesion to epithelial cells induces the release of calcium (Ca^{2+}) from intracellular stores and the appearance of novel GC receptors on the plasma membrane (22). Certain members of the Opa family of outer membrane proteins also play a role in adhesion, invasion, and tissue tropism (18, 26, 30, 52). Several receptors have been identified for Opas: heparan sulfate moieties on cell surface heparan sulfate proteoglycans (HSPG [9]), glycosaminoglycans (56), vitronectin (12), and members of the CD66 family of transmembrane glycoproteins (5, 10, 17, 59, 60). In strain MS11, binding of CD66 on phagocytic cells by Opa52 stimulates the Srk tyrosine kinases and triggers bacterial internalization via the Rac-1, PAK (p21-activated protein kinase), and Jun-N-terminal kinase pathway (21), while binding of Opa30 to HSPG on epithelial cells induces bacterial invasion via the phosphatidylcholine-specific phospholipase C and acidic sphingomyelinase cascade (16). Other bacterial components also play a role in invasion: the PI.A porin subtype (in the absence of Opa expression [55, 57]) and the bacterial lipooligosaccharide (57).

Adhesion via the type IV pilus also induces the formation of

---

* Corresponding author. Mailing address: Department of Molecular Microbiology and Immunology, L220, Oregon Health Sciences University, 3181 SW Sam Jackson Park Rd., Portland, OR 97201-3098. Phone: (503) 494-6840. Fax: (503) 494-6862. E-mail: hoppers@ohsu .edu.
† Present address: Business Development Center, Pharmacogenomic Services, Laboratory Corporation of America, Research Triangle Park, NC 27709.

cortical plaques beneath adherent bacteria (37, 39). These plaques are enriched in two Opa receptors, CD66 and HSPG; in receptor tyrosine kinases intercellular adhesion molecule 1 and epidermal growth factor receptor; and in cortical actin. Only bacteria expressing type IV pili are capable of triggering plaque formation, although the degree of plaque formation is influenced by PilT, a bacterial ATPase that is involved in DNA transformation and twitching motility (64). Based on these and other observations, an adhesion cascade model for *Neisseria* infection has been proposed (37) in which type IV pili initiate events that enhance *Neisseria* colonization of the mucosal epithelium in vivo.

The intracellular life cycle of GC is less well understood. Reports differ regarding whether intracellular GC reside within a phagosome (48, 63). Transmission electron microscopy (TEM) of infected organ cultures strongly suggests that GC replicate within epithelial cells. Few GC are seen within fallopian tube epithelial cells early in infection. In contrast, large numbers of intracellular GC are evident at late stages of infection (32). Intracellular growth studies using human epithelial cells in culture provide strong quantitative support for the TEM observations (28). Furthermore, they reveal that intracellular survival is directly correlated with the ability of the immunoglobulin A1 (IgA1) protease to alter host cell lysosomes (1, 28).

TEM of infected organ cultures demonstrates that once internalized, GC traverse the cell and exit the basal region of the cell (15, 32). Studies using polarized T84 human epithelial cell monolayers confirm these observations and demonstrate that GC transcytosis occurs without apparent damage to the monolayer (38). These studies also indicate that piliated (P$^+$) Opa$^-$ GC cross the epithelial monolayer within 36 to 48 h. Nearly identical transepithelial traversal times were reported in earlier organ culture studies (34). Piliation modulates the speed of transepithelial trafficking in a manner that is independent of its role in attachment (38). A P$^-$ strain can also traverse T84 monolayers quickly, provided it expresses Opa variants that bind the CD66 receptor (62). Finally, a mutant with a defined deletion in its *iga* (IgA1 protease) gene crossed monolayers more slowly than its isogenic wild-type (WT) parent strain and exited monolayers in fewer numbers (21a). Thus, gonococcal traversal of the epithelium is a process that is influenced by a number of virulence factors.

We are interested in identifying other molecular determinants of gonococcal transepithelial trafficking and have taken a genetic approach to accomplish this. Using polarized T84 monolayers as a model epithelial barrier, we have assayed a bank of minitransposon (mTn)-generated mutants of GC strain FA1090 (36) for isolates that traverse the monolayer more quickly than the WT parental strain. In a screen of a subset of this mutant bank, we have identified four mutants, in a P$^+$ Opa$^-$ background, that traverse monolayers significantly more quickly than the WT, P$^+$ Opa$^-$ parental strain. These mutants adhere to and invade cells normally and do not affect the integrity of the monolayer barrier. Detailed analysis of one locus revealed that it contains two genes, *fitA* and *fitB*. Interestingly, intracellular replication of the *fitA* mutant is accelerated, while its growth in vitro is normal. These results indicate that intracellular growth influences gonococcal transcellular trafficking.

MATERIALS AND METHODS

Bacterial strains and growth in liquid media. *N. gonorrhoeae* strains FA1090 (36) and MS11 variant A (MS11A) (45) were used in all experiments. Both strains are P$^+$ Opa$^-$, as judged by colony morphology and by immunoblots of total bacterial proteins using the pan-Opa monoclonal antibody 4B12 (from M.

TABLE 1. Transcytosis of WT FA1090 and mutants across polarized T84 monolayers

Strain	No. of positive assays/ total no. of assays	Avg transcytosis time (h)
A1	2/3	9
A6	2/3	4
A9	3/3	6
A10	2/4	5
A11	3/3	4
A12	3/4	5
WT	NA[a]	>24

[a] NA, nonapplicable.

Blake). GC strains were maintained on GCB agar (Difco) containing nutritional supplements and grown for 18 h at 37°C in 5% CO_2 as described previously (61). For bacterial growth assays in liquid media, GC colonies were swabbed from an 18-h agar plate and resuspended in one of the following media: GCB plus supplements I and II (61), Dulbecco modified Eagle medium (DMEM) (Gibco) plus 10% fetal calf serum (FCS; Gibco), and DMEM–F-12 (Whittaker) plus 5% FCS; the cultures were then incubated with shaking at 37°C in 5% CO_2. After 4 h of growth, the cultures were diluted to the same density with the appropriate prewarmed medium and incubated further. At various times, a portion of each culture was diluted with the appropriate medium and plated on supplemented GCB agar for enumeration of CFU.

DNA transformation. DNA transformation of GC strains was performed as described previously (47), and transformants were selected by plating bacteria on supplemented GCB agar with the appropriate antibiotics as described below.

Cloning of the GC chromosomal sequences flanking mTnEGNS into *Escherichia coli*. Chromosomal DNA was prepared from the mutants and restricted with *Mun*I and *Nhe*I. *Mun*I does not cut within mTnEGNS; *Nhe*I cuts outside the erythromycin resistance cassette (36). The restricted DNA was ligated to pHSS6 (46) that had been cut with the compatible restriction enzymes *Eco*RI and *Xba*I and dephosphorylated with shrimp alkaline phosphatase (U.S. Biochemical Corp.). The ligated DNA was electroporated into commercially available electrocompetent *E. coli* DH10B cells (Research Genetics). Transformants were selected by plating on Luria-Bertani agar plus kanamycin (60 μg/ml) and erythromycin (250 μg/ml). Plasmid DNA from kanamycin- and erythromycin-resistant (Kan^r Erm^r) colonies was purified and the inserts were excised from the plasmid vector using *Not*I. The GC sequences flanking mTnEGNS were determined by the OHSU Molecular Biology Core Facility using the primer TN3L-24 (5′ TGATAATCTCATGACCAAAATCCC 3′), which primes from the left end of the mTn towards the flanking DNA. Approximately 400 bp of nucleotide sequence was determined for each insert.

Cell culture and polarization of T84 monolayers. A431 human epidermoid carcinoma cells (from S. Schmid) were propagated in DMEM plus 10% FCS (Gibco). T84 human colonic epidermoid cells (American Type Culture Collection) were propagated in T75 flasks (Falcon) in DMEM–F-12 plus 5% FCS. T84 cells were polarized essentially as described previously (11, 29). Briefly, T84 cells (5 × 10^5/well) were plated on Transwell filters with 3-μm pores (Costar). The electrical resistance of the monolayers was measured at 3-day intervals, and monolayers with electrical resistances of >700 Ω·cm^2 were used for transcytosis assays.

Isolation of fast-trafficking mutants. Two days prior to the assay, WT FA1090 (P$^+$ Opa$^-$) was transformed as described previously (35, 47) with DNA that had been purified from pool A of an FA1090 mutant bank. This bank was derived from the random insertion of mTnEGNS, encoding resistance to erythromycin, into the FA1090 chromosome as described before (35, 36). The mutants in this bank were divided into 21 pools according to the growth rate of each mutant clone in *E. coli*, and the pools contained unique as well as overlapping mutants.

TABLE 2. Adhesion and invasion indices of WT and fast-trafficking FA1090 mutants[a]

Strain	% Cell associated	Gm^r CFU
WT	0.40 ± 0.12	2.1 × 10^{-4} ± 0.65 × 10^{-4}
A1	0.47 ± 0.15	7.8 × 10^{-5} ± 0.42 × 10^{-5}
A9	0.35 ± 0.06	3.3 × 10^{-4} ± 0.09 × 10^{-4}
A11	0.33 ± 0.05	2.0 × 10^{-4} ± 1.70 × 10^{-4}
A12	0.33 ± 0.05	2.5 × 10^{-4} ± 0.36 × 10^{-4}

[a] Determined as described in Materials and Methods. Values are the means and standard deviations from a representative experiment. Cultures were infected in triplicate.
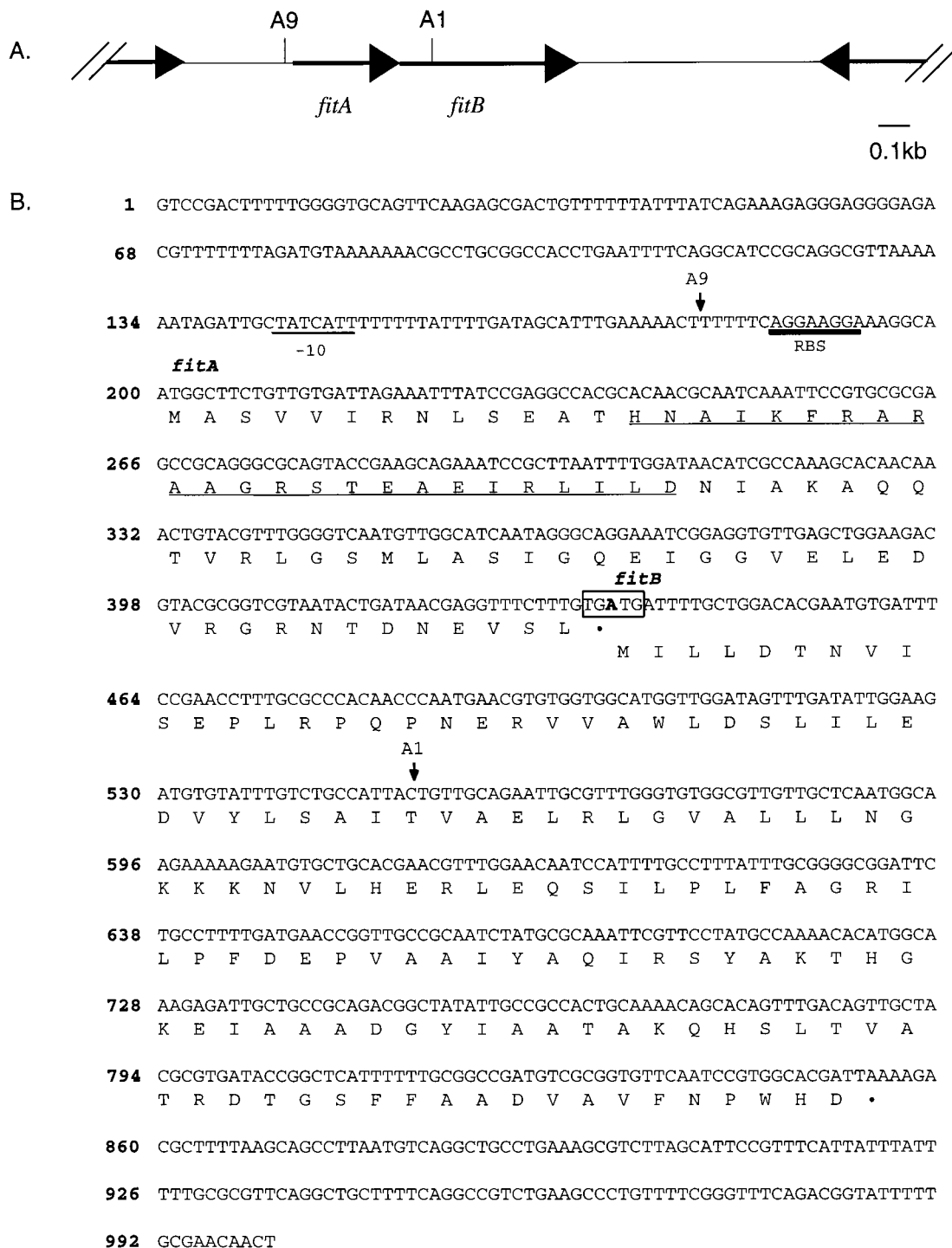
FIG. 1. Diagram of the *fit* locus. (A) Schematic representation of the orientation of the *fitA* and *fitB* genes and the upstream and downstream ORFs (arrows). The noncoding regions flanking the *fit* locus are represented by parallel lines. Sites of insertion of mTnEGNS are indicated by vertical bars; the name of the mutant appears above each bar. (B) Nucleotide and deduced amino acid sequences of the *fit* locus. The numbering of the sequence appears on the left. The RBS for *fitA* and *fitB* and the potential −10 sequence upstream of *fitA* are indicated. Arrows mark the sites of insertion of mTnEGNS, and the name of the mutant appears above each arrow. The stop codon of *fitA* and the start codon of *fitB*, where the one-nucleotide-overlap occurs, are boxed. Underlined residues in FitA indicate the potential helix-turn-helix motif.

Each pool contained mutations affecting approximately 25% of the FA1090 chromosome. Transformants were selected by plating bacteria on supplemented GCB agar plus 2 μg of Erm per ml, and the plates were incubated for 36 to 48 h at 37°C in 5% CO_2. On the day of the assay, colonies of transformants were harvested from the plates with a Dacron swab and suspended in GCB medium.

The medium was removed from the apical wells of polarized T84 monolayers (see above) and replaced with 100 μl of fresh medium supplemented with 5 μg of human transferrin (HTF; Intergen) per ml. The filter inserts containing the polarized monolayers were placed in the wells of new 24-well plates containing 0.5 ml of fresh medium. The bacterial suspensions were adjusted to 5 × 10^{8}

TABLE 3. Homology of *N. gonorrhoeae* Fit proteins to other bacterial proteins

Bacterium	Protein	% Identity (% similarity)	Protein	% Identity (% similarity)	Location
N. gonorrhoeae	FitA	100 (100)	FitB	100 (100)	Chromosome
P. syringae	StbC	46 (51)	StbB	49 (70)	Plasmid
Rhizobium sp.	Y4jj	42 (47)	Y4jK	49 (67)	Plasmid

CFU/ml, and 10 μl of each suspension was added to the apical medium of the polarized T84 monolayers. Twenty-three monolayers were infected with mutant pool A, and six monolayers were infected with WT FA1090. At various times after infection, the basal media from the wells of the infected filters were plated on supplemented GCB agar plus 2 μg of erythromycin per ml, and the plates were incubated at 37°C in 5% CO$_2$ for ~18 h to isolate transcytosed bacteria.

Bacterial adhesion, invasion, and intracellular growth assays. (i) Adhesion assays. T84 cells were seeded in 24-well plates (Falcon) at a density of 10^5/well and incubated for ~18 h at 37°C in 5% CO$_2$. Prior to the experiment, the cells were washed with prewarmed phosphate-buffered saline (PBS; Gibco). On the day of the assay, bacteria were harvested from supplemented GCB agar plates with a Dacron swab and resuspended in GCB broth, and the appropriate dilution from this suspension was used to infect cells at a multiplicity of infection (MOI) of 10. The medium was removed and discarded from a set of wells at 3.5 h postinfection, and the cells were washed six times with prewarmed PBS. The cells were lysed with GCB medium plus 0.5% saponin (Aldrich), and dilutions of the lysates were made in GCB medium and plated on supplemented GCB agar for enumeration of cell-associated CFU. At the same time points, the medium was removed from a parallel set of infected cultures, and the cells were diluted and plated on agar for enumeration of CFU. The cultures from this parallel set of wells were lysed with GCB medium plus 0.5% saponin (Aldrich), and dilutions of the lysates were also plated on agar for CFU enumeration. The sum of CFU from the medium supernatant and from the cell lysates constitutes total CFU. The adhesion index, or corrected cell-associated CFU, is calculated by dividing the number of cell-associated CFU by the number of total CFU.

(ii) Invasion assays. A431 cells were plated and infected as described above for adhesion assays. Sets of wells were washed six times with prewarmed PBS 3.5 h after infection and then incubated for 60 min with DMEM plus 10% FCS and 20 μg of gentamicin (Gibco) per ml to kill extracellular bacteria. The cultures were then washed six times with prewarmed PBS to remove gentamicin and lysed with PBS plus 0.5% saponin (Aldrich). The lysates were plated on supplemented GCB agar for enumeration of intracellular (gentamicin-resistant [Gm^r]) CFU. At the same time points, separate sets of cultures were processed for calculation of corrected cell-associated CFU as described for adhesion assays. The invasion index is calculated by dividing the number of Gm^r CFU by the corrected cell-associated CFU. All infections were performed in triplicate.

(iii) Intracellular growth assays. Approximately 18 h prior to infection, A431 cells were plated in 24-well plates at a density of 10^5/well and incubated overnight at 37°C in 5% CO$_2$. The next day, 16- to 18-h cultures of GC were harvested from supplemented GCB agar plates with a Dacron swab and resuspended in DMEM plus 10% FCS and 5 μg of HTF per ml, and the suspension was used to infect

A431 cells, which had been washed with prewarmed medium, at an MOI of 5. Infected cultures were incubated at 37°C in 5% CO$_2$ for 12 to 14 h. At the end of the infection, the cultures were washed six times with 37°C PBS and incubated with DMEM plus 10% FCS and 20 μg of gentamicin per ml for 60 min at 37°C in 5% CO$_2$. Cultures from one set of wells were lysed with GCB plus 0.5% saponin (Aldrich), and appropriate dilutions of the lysates were plated on supplemented GCB agar for CFU enumeration. The CFU from these platings are values for the 0-h time point. The remaining cultures were washed six times with 37°C PBS and incubated further in prewarmed DMEM plus 10% FCS. At each succeeding time point, one set of cultures was washed, lysed, and plated as described above. The remaining cultures were also washed with fresh prewarmed DMEM plus 10% FCS at these time points and incubated at 37°C in 5% CO$_2$ until the next time point. The intracellular CFU for each time point is the average from three infected cultures. A total of five intracellular growth assays were performed.
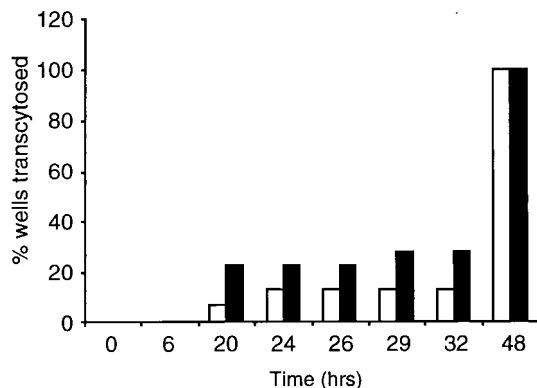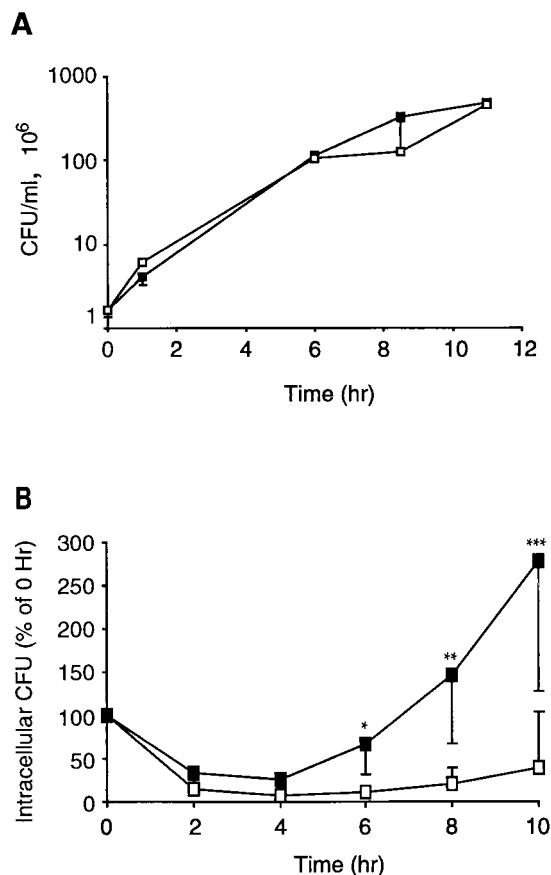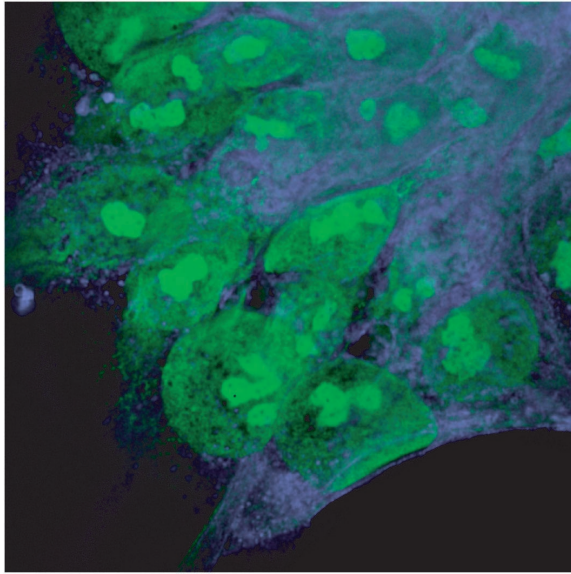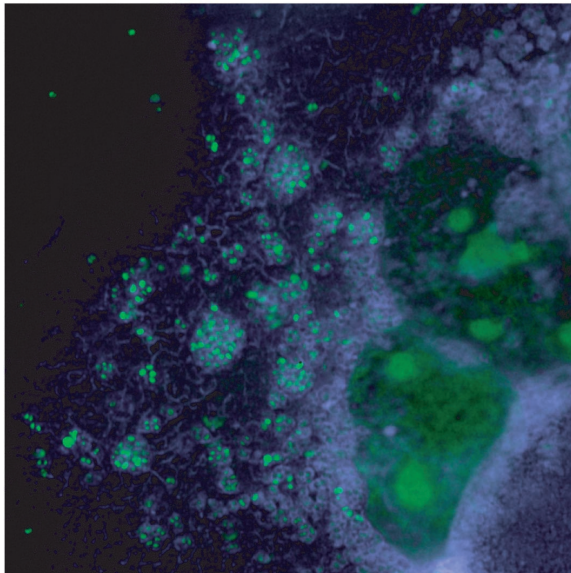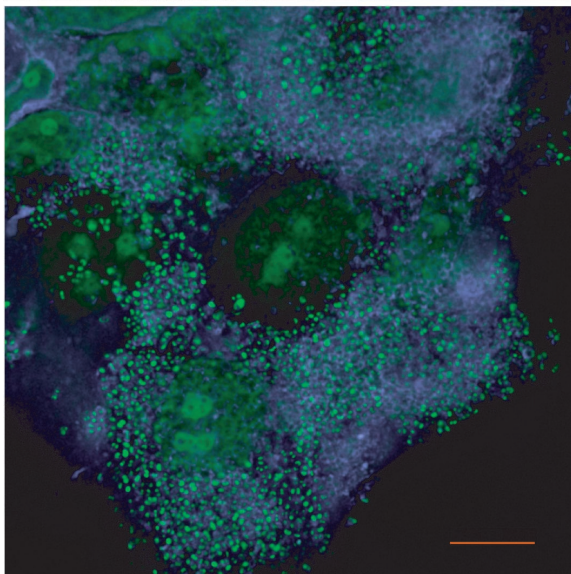

A

B

FIG. 3. Growth curves of WT MS11A (open boxes) and its isogenic *fitA* mutant (solid boxes) in DMEM plus 10% FCS (A) and in A431 human epithelial cells (B). In panel B, 0 h represents the point at which gentamicin was washed from the cultures and fresh antibiotic-free medium was added. For WT CFU, upper bounds with 95% confidence limits are shown. For *fitA* CFU, lower bounds with 95% confidence limits are shown. Single, double, and triple asterisks indicate that Student's paired one-tailed *t* test was performed for the values from the two strains from the 6-, 8-, and 10-h time points, respectively. In each case, *P* < 0.05.

FIG. 2. Transcytosis times of WT MS11A and the MS11A *fitA* mutant. Polarized T84 monolayers were infected with WT or *fitA* bacteria, both P$^+$ Opa$^-$. At the indicated times, the presence of bacteria in the basal medium (i.e., exocytosed bacteria) was determined as described in Materials and Methods. The results are the sum of two independent experiments. A total of 16 polarized monolayers were infected with WT bacteria (white bars), and 18 monolayers were infected with *fitA* bacteria (black bars).

UI

WT

fitA

Transcytosis assays. Transcytosis assays were performed as described elsewhere (21a, 38). On the day of the assay, the medium from the apical wells of polarized T84 monolayers (see above) was removed and replaced with 100 μl of fresh medium supplemented with 5 μg of HTF per ml. The filter inserts containing the polarized monolayers were placed in the wells of fresh 24-well plates containing 0.5 ml of medium per well. The bacteria were suspended in GCB broth at a density of 5×10^8 CFU/ml, and 10 μl of this suspension was added to the medium in the apical wells of polarized T84 monolayers. Infected monolayers were incubated at 37°C in 5% CO_2. At defined intervals, the infected filter inserts were transferred to new 24-well plates containing fresh basal medium and incubated further. The previously used 24-well plates were incubated further at 37°C in 5% CO_2 to assess the presence of bacteria in the basal medium. Bacterial growth resulted in an increase in turbidity and a pH (color) change of the medium.

Fluorescence microscopy. T84 cells were seeded in six-well tissue culture plates (Falcon) containing ethanol-washed, autoclaved sterile glass coverslips (one per well) (Fisher no. 1.5 18- by 18-mm coverslips). Cells grew to approximately 50% confluency in 36 h in DMEM–F-12 containing 5% FCS at 37°C in 5% CO_2. At this time, cells were given fresh, prewarmed media. WT and *fitA* MS11A organisms were harvested from GCB agar with a Dacron swab and suspended in GCB broth. Approximately 10^7 CFU from these suspensions was used to inoculate each culture well. Plates were incubated at 37°C in 5% CO_2 for 18 h.

The coverslips were carefully removed from the culture medium and washed vigorously three times with PBS. Cells were then fixed in freshly prepared 4% paraformaldehyde in PBS for 10 min at room temperature (RT). Coverslips were rinsed three times in PBS and then blocked in 3% normal goat serum (NGS; Life Technologies) in PBS for 30 min at RT. The coverslips were incubated for 1 h at RT with a rabbit polyclonal antibody to whole GC (38) that had been diluted 1:250 in 3% NGS in PBS. They were then transferred to fresh plates, washed three times in PBS, and subsequently incubated in goat anti-rabbit Alexa-488-conjugated antibody (Molecular Probes) diluted 1:2,000 in 3% NGS in PBS.

Coverslips were again washed three times in PBS. Propidium iodide (PI) (1-mg/ml solution in water; Molecular Probes) was diluted to 5 μg/ml, and 1-(4-trimethylammoniumphenyl)-6-phenyl-1,3,5-hexatriene–*p*-toluenesulfonate (TMA-DPH; Molecular Probes) was diluted to 0.25 mg/ml in PBS containing 0.05% (wt/vol) saponin (Aldrich). Coverslips were incubated in this solution for 10 min at RT and then washed three times with PBS. Each coverslip was mounted on a slide using Fluoromount-G (Southern Biotechnology).

Images were captured using a DeltaVision workstation with a Nikon TE-200 platform, courtesy of Applied Precision, Inc., Seattle, Wash. Complete series of images were taken through the entire width of the sample at 0.2-μm z-steps using a Plan-Apo 60× 1.40 NA (numerical aperture) oil immersion objective. Each set was processed using iterative deconvolution algorithms in the DeltaVision 2.0 software package. Single optical sections were selected as representative of intracellular bacterial populations based on the presence of nuclei and lack of staining of bacteria by the fluorescent antibody. Images were processed using the DeltaVision 2.0 and Adobe Photoshop 5.0 software.

Nucleotide sequence accession number. The nucleotide sequence of the *fit* locus has been deposited in GenBank with accession number AF200716.

RESULTS

Isolation of fast-trafficking FA1090 mutants. We wished to isolate gonococcal mutants that traverse polarized T84 monolayers more quickly than the WT FA1090 strain. Such mutants, unlike slow-trafficking mutants or mutants that fail to transcytose, are relatively easy to obtain because of the length of time taken by P^+ Opa^- GC to traverse the monolayer (21a, 38). Some mutations that result in a fast-trafficking phenotype may be in control genes, and understanding the control of transcellular trafficking could yield information that may not be obtained by other experimental approaches. The FA1090 strain was chosen for these experiments because the sequence of its genome is nearly completely determined and readily available (http://www.genome.ou.edu/gono.html), thus accelerating the identification of mTn-mutagenized loci.

The construction of a bank of FA1090 mutants and the isolation of pilin antigenic-variation mutants from this bank

have been described in detail (35, 36). This bank was derived from the random insertion of mTnEGNS, encoding resistance to erythromycin, into the FA1090 chromosome. The mutants in this bank were divided into 21 pools according to the growth rate of each mutant clone in *E. coli*, and the pools contained unique as well as overlapping mutants. Each pool contained mutations affecting approximately 25% of the FA1090 chromosome. Mutant pool A was used to infect the apical wells of polarized T84 monolayers, and at 2-h intervals, exocytosed bacteria were isolated by plating the basal medium on GCB agar plus erythromycin. As a control, the WT FA1090 strain was used to inoculate a parallel set of monolayers, and exocytosed WT bacteria were monitored by plating the basal medium on GCB agar. All strains were P^+ Opa^- as judged by the morphology of the colonies in the plate culture used for infection as well as by immunoblots of total bacterial proteins.

Infection of 23 polarized T84 monolayers with pool A of the FA1090 mutant bank yielded six mutants, A1, A6, A9, A10, A11, and A12, that crossed T84 monolayers within 10 h after infection. These mutants were isolated from different infected monolayers. As expected, WT FA1090 took over 24 h to cross the monolayers (data not shown). The mutants were analyzed in additional assays. All six mutants maintained their fast-trafficking phenotype (Table 1). For instance, in three of four assays, mutant A12 crossed T84 monolayers more quickly than the WT strain, taking, on average, 6 h to cross the barrier. In contrast, WT FA1090 took over 24 h to traverse the monolayer. After 24 h of infection, the electrical resistance of all infected monolayers was within 90% of starting values (data not shown), indicating that the mutants had no detectable effect on the integrity of the monolayer barrier.

Backcrosses with WT FA1090. To determine whether the mTn disruptions are responsible for the aberrant transcytosis phenotypes, chromosomal DNA from A1, A6, A9, A10, A11, and A12 was used to transform WT P^+ Opa^- FA1090. All Erm^r transformants from these backcrosses traversed polarized T84 monolayers more quickly than the WT FA1090 strain (data not shown). Thus, the fast-trafficking phenotype of the mutants is directly linked to the mTn insertions and not to mutations at secondary sites.

Characterization of the mTn-disrupted sites. Chromosomal fragments from the six mutants containing mTnEGNS and their flanking DNA were cloned into *E. coli* in the pHSS6 vector (46). Approximately 400 bp of GC sequence flanking one end of mTnEGNS in each insert was determined and used to search the *N. gonorrhoeae* FA1090 Genome Database (http://www.genome.ou.edu/gono.html). In mutants A1, A6, and A10, mTnEGNS had inserted at the same site and in the same orientation. As noted above, these mutants were isolated from different infected monolayers. Thus, the same mutant in pool A had been isolated three times independently in the same experiment. In A1 and A9, mTnEGNS had inserted in opposite orientation into the same locus 370 bp apart (see below). Thus, the mutations in A1 and A9 are closely linked. The mutations in A11 and A12 are in different regions of the chromosome. In all mutants, the loci inactivated by mTnEGNS have no homology to known gonococcal virulence factors.

Adhesion and invasion assays. To determine whether the fast-trafficking phenotype of the mutants is due to an increased

---

FIG. 4. Fluorescence microscopy of T84 monolayers. T84 cells were infected with WT MS11A (WT) or the MS11A *fitA* mutant (*fitA*) or left uninfected (UI). The cultures were fixed with formaldehyde and stained with a polyclonal anti-GC antibody to visualize extracellular bacteria. They were then permeabilized and stained with TMA-DPH to visualize total cellular membranes and with PI to visualize bacterial DNA and the nucleus. Left panels, T84 cells visualized for membranes (blue) and nucleic acids (green); right panels, the same field of cells visualized for adhered bacteria (grey). Samples were imaged using the DeltaVision Restoration Microscopy System, courtesy of Applied Precision, Inc. Magnification, ×1,800. Scale bar (red), 10 μm.

ability to attach to or invade cells, adhesion and invasion assays were performed on the backcrossed A1, A9, A11, and A12 mutants and the WT FA1090 strain. Adhesion assays were performed with T84 cells; invasion assays were performed with A431 cells, as T84 cells secrete large amounts of mucus, which decreases the effectiveness of gentamicin in killing extracellular bacteria (21a). The mutants adhered to and invaded epithelial cells no more quickly than the WT strain (Table 2), indicating that the rapid-transcytosis phenotype of mutants A1, A9, A11, and A12 is not due to accelerated adhesion or invasion.

Sequence analysis of the *fit* locus. In mutants A1 and A9, the mTn had inserted into the same locus (Fig. 1A). This locus, which has been named *fit*, for fast intracellular trafficker, contains two open reading frames (ORFs). *fitA* is 234 nucleotides long and is preceded by a ribosome binding site (RBS) and a possible −10 sequence, but not by any identifiable −35 sequence. The deduced FitA polypeptide is 78 amino acids, with a predicted molecular weight (MW) of 8.6. *fitB* is 417 nucleotides; it is preceded by an RBS but not by a readily identifiable −10 or −35 sequence. The deduced FitB polypeptide is 139 amino acids, with a predicted MW of 15.3. *fitA* overlaps *fitB* by one nucleotide; the last nucleotide of the *fitA* translation termination codon (TGA) is the first nucleotide of the *fitB* initiation codon (ATG [Fig. 1B]). This overlapping arrangement is often observed in genes that are translationally coupled (41, 49). In A9, the mTn had inserted between the −10 region and the RBS of *fitA*. In A1, the mTn had inserted in the opposite orientation, between bp +116 and +117 in *fitB*. Thus, two mTn insertions at different sites within the same locus resulted in mutants with a fast-trafficking phenotype. These results lend additional support to the role of the *fit* locus in GC transepithelial trafficking.

The *fit* locus is separated from the nearest upstream ORF by >300 bp and from the nearest downstream ORF by >800 bp (Fig. 1A). The upstream ORF is in the same orientation as the *fit* locus, while the downstream ORF is in the opposite orientation. It is therefore unlikely that the mTnEGNS insertions in the *fit* locus altered expression of these surrounding ORFs. Moreover, no DNA rearrangements in the *fit* region have been detected by Southern hybridization of chromosomal DNA from mutants A1 and A9 using a *fitA* or *fitB* probe (data not shown). Thus, the fast-trafficking phenotype of these mutants is due to the interruptions in the *fit* locus.

The predicted Fit proteins do not have the classical signal sequence recognized by the general secretory pathway of gram-negative bacteria (43). FitA has a potential helix-turn-helix motif that is found in many bacterial DNA-binding proteins (7). Homologues of *fitA* and *fitB* exist in other bacteria, with those from *Rhizobium meliloti* and *Pseudomonas syringae* being the most closely related (Table 3). Both the *Pseudomonas* and *Rhizobium fitA* and *fitB* homologues (*stbC* and *stbB* in *Pseudomonas* and *y4jJ* and *y4jK* in *Rhizobium*) reside on plasmids (13, 20). Like *fitA* and *fitB*, each set of homologues also overlaps by one nucleotide. The function of the *Pseudomonas* and *Rhizobium fitA* and *fitB* homologues is unknown. *fit* sequences are not present in the genome of *Neisseria meningitidis* strain Z2491 or MC58 (http://www.sanger.ac.uk/projects/N.meningitidis/, http://www.tigr.org/tdb/mdb/mdb.html). *N. meningitidis* shares over 80% nucleotide sequence homology with GC and is the only other pathogenic member of the genus *Neisseria*. This finding suggests that the *fit* genes have a specialized function in GC pathogenesis.

Backcrossing of the FA1090 *fitA* mutation into the MS11 background. The FA1090 A9 mutant, with the mTn insertion at the noncoding 5′ region of *fitA*, was backcrossed into the

genetic background of strain MS11A. Transcytosis assays were performed on WT MS11A and one Erm^r P$^+$ Opa$^-$ transformant from the backcross (Fig. 2). At 6 to 20 h postinfection, the MS11A *fit* mutant had traversed 22% of the monolayers (4 of 18); at 26 to 29 h, it had crossed 28% of the monolayers (6 of 18). In contrast, WT MS11A had crossed 6.25% of the monolayers (1 of 16) at 6 to 20 h and 12.5% of the monolayers (2 of 16) at 26 to 29 h. By 36 to 48 h, both *fit* and WT bacteria had crossed all monolayers. Taken together, these results demonstrate that mutations in *fitA* in two GC isolates result in similar fast-trafficking phenotypes.

Growth of the *fitA* mutant. In an attempt to determine the function of the *fit* locus in transepithelial trafficking, the growth of the *fitA* mutant under a variety of conditions was examined. The *fitA* mutant in the MS11A genetic background was used for these and subsequent experiments because extensive data have been gathered on the interactions of this strain with epithelial cells. Growth of *fitA* bacteria in liquid media was first studied. The WT and *fitA* strains were inoculated into supplemented GCB broth, DMEM plus 10% FCS, and DMEM–F-12 plus 10% FCS, the medium used for propagating T84 monolayers. Cultures were incubated at 37°C in 5% CO_2, and at various times, samples were plated on GCB agar for CFU enumeration. The *fitA* mutant and the isogenic WT strain grew equally well in all media tested. The growth curves from the experiment with DMEM plus 10% FCS are shown in Fig. 3A. The *fitA* mutant and WT GC also grow equally well on agar plates (data not shown). Thus, there is no altered growth phenotype for the *fit* mutant in vitro.

The MS11A *fitA* mutant was also examined for growth within A431 epithelial cells. A431 cells were infected for 14 to 16 h with WT or *fitA* bacteria at an MOI of 5. Extracellular bacteria were then killed by treatment of the cultures with gentamicin, and the cultures were assayed for intracellular CFU at various times after removal of the antibiotic. Results indicate that the number of intracellular CFU from both WT and *fitA* bacteria decreased for a period of time after removal of gentamicin (Fig. 3B). This decrease in viable intracellular CFU has been observed with another GC strain (28). The numbers of viable intracellular *fitA* mutants began to rise 4 h after removal of gentamicin and by the end of the incubation period had increased threefold. The number of intracellular WT bacteria also increased but much more slowly than the number of *fitA* bacteria.

Replication of the MS11A *fitA* mutant within T84 cells was also examined by fluorescence microscopy. T84 cells grown on coverslips were infected for 18 h with WT or *fitA* bacteria and then washed extensively to remove nonadherent bacteria. The infected cultures were stained with a polyclonal antibody directed to total GC proteins and then permeabilized and stained with TMA-DPH, a lipophilic fluorescent dye which is incorporated into cellular membranes, and PI, which is incorporated into nuclear and bacterial nucleic acids. Staining infected cultures with the anti-GC antibody before permeabilization permits the detection only of extracellular bacteria. Staining with PI after permeabilization allows visualization of all bacteria as well as the nucleus. This differential staining approach therefore allows the discrimination of extracellular and intracellular bacteria.

Numerous punctate PI signals were observed within the focal planes of the interiors of infected cells (Fig. 4, lower left panel); these signals were absent from uninfected cells (Fig. 4, upper left panel). These signals therefore originated from GC. Few bacteria were stained by the anti-GC antibody (Fig. 4, right panels); thus, the bacteria in the cultures were mostly intracellular. The *fitA* mutant appeared in greater numbers

within T84 cells than the WT strain. Such differences in intracellular numbers between the WT and *fitA* strains were also observed in infected polarized T84 monolayers (data not shown). Thus, intracellular growth of the *fitA* mutant is accelerated in both T84 and A431 epithelial cells.

DISCUSSION

Using polarized T84 human epithelial monolayers as a model epithelial barrier, we have screened a portion of an mTn-generated FA1090 mutant bank for fast-trafficking isolates. Four such mutants, defining three distinct loci, were isolated. These mutants, which are P$^+$ Opa$^-$, traversed polarized T84 monolayers more quickly than the WT P$^+$ Opa$^-$ FA1090 strain (Table 1). The mutant phenotype is due to the mTn insertions, as backcrosses of the mutations into WT FA1090 yielded mutants with a similar fast-trafficking phenotype. The mutants adhered to and invaded cells normally (Table 2), and the electrical resistance of infected monolayers was high after the bacteria had exited the monolayer (data not shown). Thus, the fast-trafficking phenotype is not due to an enhancement of bacterial adherence or invasion or to a decrease in the integrity of the cellular barrier. Taken together, these results indicate that the mutants were affected in the process of transepithelial trafficking.

Two mutants, A1 and A9, were examined in detail. In these mutants, the mTn had inserted in opposite orientation into the same locus 370 bp apart. This locus, termed *fit*, contains two ORFs, *fitA* and *fitB* (Fig. 1B). In A9, the mTn had inserted 6 bp upstream of the RBS of *fitA*; in A1, the mTn had inserted at position +116 of *fitB* (Fig. 1B). Backcrossing of the A9 mutation into a WT P$^+$ Opa$^-$ MS11A strain also resulted in a mutant with a similar fast-trafficking phenotype (Fig. 2). These results argue strongly for the importance of the *fit* locus in transepithelial trafficking.

The chain termination codon of *fitA* overlaps the initiation codon of *fitB* by one nucleotide. A similar situation exists for the neisserial *lbpA* and *lbpB* genes, which encode outer membrane proteins that bind human lactoferrin (2, 3, 42). *lbpB* precedes *lbpA*, and the two genes also overlap. In this case, the T in the *lbpB* TGA chain termination codon is the T in the *lbpA* ATG initiation codon. The two genes are transcribed as a polycistronic message and are at least partially translationally coupled (4, 27). Whether expression of *fitA* and *fitB* is similarly controlled remains to be tested.

The deduced FitA and FitB proteins are predicted to have MWs of 8.6 and 15.3, respectively. Neither protein has a signal sequence recognized by the general secretory pathway of gram-negative bacteria (43). FitA has a potential helix-turn-helix motif that is characteristic of bacterial DNA-binding proteins (6). The lack of a secretion signal in the Fit proteins and the possibility that FitA may be a DNA-binding protein are consistent with our expectation that at least some of the mutants isolated from this transcytosis assay would be affected in control genes.

The MS11A *fitA* mutant grew normally in the three liquid media tested (Fig. 3A) and on agar plates. However, its growth within epithelial cells was very different from that of the WT strain (Fig. 3B). In A431 epithelial cell culture assays, the number of intracellular *fitA* and WT bacteria decreased over a period of time after removal of gentamicin from the infected cultures (0 h). The number of intracellular *fitA* bacteria began to rise at 4 h and by 10 h had increased more than threefold. The number of intracellular WT bacteria also increased, but the rise in CFU began later and continued at a slower pace. Fluorescence microscopy of infected T84 cells supported these

observations; it revealed that *fitA* bacteria were much more numerous within polarized (data not shown) and unpolarized (Fig. 4) T84 cells than WT bacteria. Taken together, these results demonstrate that the MS11A *fitA* mutant grows aberrantly in at least two epithelial cell lines; in contrast, it grows normally in media in the absence of epithelial cells.

In summary, these results strongly suggest that altered intracellular growth of GC is one consequence of mutations in the *fit* locus. They suggest that expression of this locus is regulated and that it may respond to a stimulus that GC encounter when cultured with epithelial cells. How the Fit proteins function in relation to gonococcal growth within epithelial cells and how *fit* expression is controlled are under investigation.

GC transepithelial trafficking is likely to be a complicated process involving the participation of a number of bacterial genes. Several studies indicate that early interactions of GC with the host cell plasma membrane influence subsequent transepithelial trafficking. One study strongly suggests that pilus-mediated interactions with the host cell, possibly related to the invasion process, can influence gonococcal traversal of polarized T84 monolayers (38). In a similar vein, P$^-$ MS11 expressing Opa variants that bind the CD66 receptor crosses T84 monolayers rapidly, in contrast to strains that express no Opas or Opa variants with different receptor specificities (62). Thus, CD66-mediated gonococcal interactions with the host cell plasma membrane can also modulate subsequent bacterial transcellular trafficking. The secreted neisserial IgA1 protease also plays a role in GC transcytosis: an *iga* null mutant in a P$^+$ Opa$^-$ background crosses monolayers more slowly than the WT parental strain in early stages of infection and exists monolayers in fewer numbers (21a). That the IgA1 protease promotes survival of GC within epithelial cells (28) may explain why *iga* mutants exit the monolayer in fewer numbers than the WT parent strain. It is also consistent with the results in this report demonstrating a relationship between intracellular growth and transepithelial trafficking.

How intracellular growth of GC affects transcytosis is unclear. Several possible scenarios can be proposed. (i) Reports differ regarding whether intracellular GC reside within phagosomes (48, 63). The *fitA* mutant may rapidly enter a compartment that permits transcytosis. (ii) The coding regions of many gonococcal virulence genes contain pentanucleotide repeats (e.g., the *opa* gene family). The expression of this class of genes is phase variable and governed by slipped-strand mispairing of the repeat regions at replication forks (40, 51). Accelerated intracellular replication of the *fit* mutant may increase the phase switching of genes that modulate transcytosis. Supporting this hypothesis is the observation that GC expressing the *opa52* gene crossed polarized T84 monolayers rapidly, in contrast to variants that express no *opa* or those that express other *opa* variants, which failed to cross the monolayers within the time frame of the experiment (62). (iii) Finally, it is possible that the simple increase in the number of intracellular GC may be enough to accelerate transcellular trafficking, regardless of the transcytosis mechanism. Of the three explanations, the last seems the most unlikely. Studies to date indicate that the trafficking of cellular components and trafficking of bacteria within cells are tightly controlled processes that require the participation of specific cellular proteins and structures (14, 31, 44, 50, 54, 58). It will be interesting to determine the molecular basis of the relationship between intracellular growth and transcytosis.

REFERENCES

1. **Ayala, P., L. Lin, S. Hopper, M. Fukuda, and M. So.** 1998. Infection of epithelial cells by pathogenic neisseriae reduces the levels of multiple lysosomal constituents. Infect. Immun. **66:**5001–5007.

2. **Biswas, G. D., and P. F. Sparling.** 1995. Characterization of *lbpA*, the structural gene for a lactoferrin receptor in *Neisseria gonorrhoeae*. Infect. Immun. **63:**2958–2967.

3. **Bonnah, R. A., R. Yu, and A. B. Schryvers.** 1995. Biochemical analysis of lactoferrin receptors in the *Neisseriaceae*: identification of a second bacterial lactoferrin receptor protein. Microb. Pathog. **19:**285–297.

4. **Bonnah, R. A., and A. B. Schryvers.** 1998. Preparation and characterization of *Neisseria meningitidis* mutants deficient in production of the human lactoferrin-binding proteins LbpA and LbpB. J. Bacteriol. **180:**3080–3090.

5. **Bos, M. P., F. Grunert, and R. J. Belland.** 1997. Differential recognition of members of the carcinoembryonic antigen family by Opa variants of *Neisseria gonorrhoeae*. Infect. Immun. **65:**2353–2361.

6. **Brennan, R. G., and B. W. Matthews.** 1989. The helix-turn-helix DNA binding motif. J. Biol. Chem. **264:**1903–1906.

7. **Brennan, R. G., and B. W. Matthews.** 1989. Structural basis of DNA-protein recognition. Trends Biochem. Sci. **14:**286–290.

8. **Buchanan, T. M., W. A. Pearce, G. K. Schoolnik, and R. J. Arko.** 1977. Protection against infection with *Neisseria gonorrhoeae* by immunization with outer membrane protein complex and purified pili. J. Infect. Dis. **136**(Suppl.)**:**S132–S137.

9. **Chen, T., R. J. Belland, J. Wilson, and J. Swanson.** 1995. Adherence of pilus− Opa+ gonococci to epithelial cells *in vitro* involves heparan sulfate. J. Exp. Med. **182:**511–517.

10. **Chen, T., F. Grunert, A. Medina-Marino, and E. C. Gotschlich.** 1997. Several carcinoembryonic antigens (CD66) serve as receptors for gonococcal opacity proteins. J. Exp. Med. **185:**1557–1564.

11. **Dharmsathaphorn, K., and J. L. Madara.** 1990. Established intestinal cell lines as model systems for electrolyte transport studies. Methods Enzymol. **192:**354–389.

12. **Duensing, T. D., and J. P. van Putten.** 1997. Vitronectin mediates internalization of *Neisseria gonorrhoeae* by Chinese hamster ovary cells. Infect. Immun. **65:**964–970.

13. **Freiberg, C., R. Fellay, A. Bairoch, W. J. Broughton, A. Rosenthal, and X. Perret.** 1997. Molecular basis of symbiosis between *Rhizobium* and legumes. Nature **387:**394–401.

14. **Gerst, J. E.** 1999. SNAREs and SNARE regulators in membrane fusion and exocytosis. Cell. Mol. Life Sci. **55:**707–734.

15. **Gorby, G. L., E. N. Robinson, Jr., L. R. Barley, C. M. Clemens, and Z. A. McGee.** 1988. Microbial invasion: a covert activity? Can. J. Microbiol. **34:**507–512.

16. **Grassme, H., E. Gulbins, B. Brenner, K. Ferlinz, K. Sandhoff, K. Harzer, F. Lang, and T. F. Meyer.** 1997. Acidic sphingomyelinase mediates entry of *N. gonorrhoeae* into nonphagocytic cells. Cell **91:**605–615.

17. **Gray-Owen, S. D., C. Dehio, A. Haude, F. Grunert, and T. F. Meyer.** 1997. CD66 carcinoembryonic antigens mediate interactions between Opa-expressing *Neisseria gonorrhoeae* and human polymorphonuclear phagocytes. EMBO J. **16:**3435–3445.

18. **Gray-Owen, S. D., D. R. Lorenzen, A. Haude, T. F. Meyer, and C. Dehio.** 1997. Differential Opa specificities for CD66 receptors influence tissue interactions and cellular response to *Neisseria gonorrhoeae*. Mol. Microbiol. **26:**971–980.

19. **Griffiss, J. M., C. J. Lammel, J. Wang, N. P. Dekker, and G. F. Brooks.** 1999. *Neisseria gonorrhoeae* coordinately uses pili and Opa to activate HEC-1-B cell microvilli, which causes engulfment of the gonococci. Infect. Immun. **67:**3469–3480.

20. **Hanekamp, T., D. Kobayashi, S. Hayes, and M. M. Stayton.** 1997. Avirulence gene D of *Pseudomonas syringae* pv. tomato may have undergone horizontal gene transfer. FEBS Lett. **415:**40–45.

21. **Hauck, C. R., T. F. Meyer, F. Lang, and E. Gulbins.** 1998. CD66-mediated phagocytosis of Opa52 *Neisseria gonorrhoeae* requires a Src-like tyrosine kinase- and Rac1-dependent signalling pathway. EMBO J. **17:**443–454.

21a.**Hopper, S., B. Vasquez, A. Merz, S. Clary, J. S. Wilbur, and M. So.** 2000. Effects of the immunoglobulin A1 Protease on *Neisseria gonorrhoeae* trafficking across polarized T84 epithelial monolayers. Infect. Immun. **68:**906–911.

22. **Kallstrom, H., M. S. Islam, P. O. Berggren, and A. B. Jonsson.** 1998. Cell signaling by the type IV pili of pathogenic *Neisseria*. J. Biol. Chem. **273:**21777–21782.

23. **Kallstrom, H., M. K. Liszewski, J. P. Atkinson, and A. B. Jonsson.** 1997. Membrane cofactor protein (MCP or CD46) is a cellular pilus receptor for pathogenic *Neisseria*. Mol. Microbiol. **25:**639–647.

24. **Kellogg, D. S., Jr., I. R. Cohen, L. C. Norins, A. L. Schroeter, and G. Reising.** 1968. *Neisseria gonorrhoeae*. II. Colonial variation and pathogenicity during 35 months in vitro. J. Bacteriol. **96:**596–605.

25. **Kellogg, D. S., Jr., W. L. Peacock, Jr., W. E. Deacon, L. Brown, and C. I. Pirkle.** 1963. *Neisseria gonorrhoeae*. I. Virulence genetically linked to clonal variation. J. Bacteriol. **85:**1274–1279.

26. **Kupsch, E. M., B. Knepper, T. Kuroki, I. Heuer, and T. F. Meyer.** 1993. Variable opacity (Opa) outer membrane proteins account for the cell tropisms displayed by *Neisseria gonorrhoeae* for human leukocytes and epithelial cells. EMBO J. **12:**641–650.

27. **Lewis, L. A., K. Rohde, M. Gipson, B. Behrens, E. Gray, S. I. Toth, B. A. Roe, and D. W. Dyer.** 1998. Identification and molecular analysis of *lbpBA*, which encodes the two-component meningococcal lactoferrin receptor. Infect. Immun. **66:**3017–3023.

28. **Lin, L., P. Ayala, J. Larson, M. Mulks, M. Fukuda, S. R. Carlsson, C. Enns, and M. So.** 1997. The *Neisseria* type 2 IgA1 protease cleaves LAMP1 and promotes survival of bacteria within epithelial cells. Mol. Microbiol. **24:**1083–1094.

29. **Madara, J. L., J. Stafford, K. Dharmsathaphorn, and S. Carlson.** 1987. Structural analysis of a human intestinal epithelial cell line. Gastroenterology **92:**1133–1145.

30. **Makino, S., J. P. van Putten, and T. F. Meyer.** 1991. Phase variation of the opacity outer membrane protein controls invasion by *Neisseria gonorrhoeae* into human epithelial cells. EMBO J. **10:**1307–1315.

31. **Mays, R. W., W. J. Nelson, and J. A. Marrs.** 1995. Generation of epithelial cell polarity: roles for protein trafficking, membrane-cytoskeleton, and E-cadherin-mediated cell adhesion. Cold Spring Harbor Symp. Quant. Biol. **60:**763–773.

32. **McGee, Z., and R. Horn.** 1988. Phagocytosis of gonococci by nonprofessional phagocytic cells. Rev. Infect. Dis. **10:**158–161.

33. **McGee, Z. A., and M. L. Woods, Jr.** 1987. Use of organ cultures in microbiological research. Annu. Rev. Microbiol. **41:**291–300.

34. **McGee, Z. A., A. P. Johnson, and D. Taylor-Robinson.** 1981. Pathogenic mechanisms of *Neisseria gonorrhoeae*: observations on damage to human Fallopian tubes in organ culture by gonococci of colony type 1 or type 4. J. Infect. Dis. **143:**413–422.

35. **Mehr, I. J., and H. S. Seifert.** 1998. Differential roles of homologous recombination pathways in *Neisseria gonorrhoeae* pilin antigenic variation, DNA transformation and DNA repair. Mol. Microbiol. **30:**697–710.

36. **Mehr, I. J., and H. S. Seifert.** 1997. Random shuttle mutagenesis: gonococcal mutants deficient in pilin antigenic variation. Mol. Microbiol. **23:**1121–1131.

37. **Merz, A. J., C. A. Enns, and M. So.** 1999. Type IV pili of pathogenic *Neisseriae* elicit cortical plaque formation in epithelial cells. Mol. Microbiol. **32:**1316–1332.

38. **Merz, A. J., D. B. Rifenbery, C. G. Arvidson, and M. So.** 1996. Traversal of a polarized epithelium by pathogenic *Neisseriae*: facilitation by type IV pili and maintenance of epithelial barrier function. Mol. Med. **2:**745–754.

39. **Merz, A. J., and M. So.** 1997. Attachment of piliated, Opa− and Opc− gonococci and meningococci to epithelial cells elicits cortical actin rearrangements and clustering of tyrosine-phosphorylated proteins. Infect. Immun. **65:**4341–4349.

40. **Murphy, G., T. Connell, D. Barritt, M. Koomey, and J. Cannon.** 1989. Phase variation of gonococcal protein II: regulation of gene expression by slipped-strand mispairing of a repetitive DNA sequence. Cell **56:**539–547.

41. **Pavelka, M. S., Jr., L. F. Wright, and R. P. Silver.** 1991. Identification of two genes, *kpsM* and *kpsT*, in region 3 of the polysialic acid gene cluster of *Escherichia coli* K1. J. Bacteriol. **173:**4603–4610.

42. **Pettersson, A., A. Maas, and J. Tommassen.** 1994. Identification of the *iroA* gene product of *Neisseria meningitidis* as a lactoferrin receptor. J. Bacteriol. **176:**1764–1766.

43. **Pugsley, A. P.** 1993. The complete general secretory pathway in gram-negative bacteria. Microbiol. Rev. **57:**50–108.

44. **Sansonetti, P. J., J. Mounier, M. C. Prevost, and R. M. Mege.** 1994. Cadherin expression is required for the spread of *Shigella flexneri* between epithelial cells. Cell **76:**829–839.

45. **Segal, E., E. Billyard, M. So, S. Storzbach, and T. F. Meyer.** 1985. Role of chromosomal rearrangement in *N. gonorrhoeae* pilus phase variation. Cell **40:**293–300.

46. **Seifert, H. S., E. Y. Chen, M. So, and F. Heffron.** 1986. Shuttle mutagenesis: a method of transposon mutagenesis for *Saccharomyces cerevisiae*. Proc. Natl. Acad. Sci. USA **83:**735–739.

47. **Seifert, H. S., and M. So.** 1991. Genetic systems in pathogenic *Neisseriae*. Methods Enzymol. **204:**342–357.

48. **Shaw, J. H., and S. Falkow.** 1988. Model for invasion of human tissue culture cells by *Neisseria gonorrhoeae*. Infect. Immun. **56:**1625–1632.

49. **Silver, R. P., R. P. Annunziato, M. S. Pavelka, R. P. Pigeon, L. F. Wright, and D. E. Wunder.** 1993. Genetic and molecular analyses of the polysialic acid gene cluster of *Escherichia coli* K1, p. 59–71. *In* J. Roth, U. Rutishauser, and F. A. Troy (ed.), Polysialic acid: from microbes to man. Birkhauser Verlag, Basel, Switzerland.

50. **Song, W., G. Apodaca, and K. Mostov.** 1994. Transcytosis of the polymeric immunoglobulin receptor is regulated in multiple intracellular compartments. J. Biol. Chem. **269:**29474–29480.

51. **Stern, A., P. Nickel, T. F. Meyer, and M. So.** 1984. Opacity determinants of *Neisseria gonorrhoeae*: gene expression and chromosomal linkage to the gonococcal pilus gene. Cell **37:**447–456.

52. **Swanson, J.** 1992. Growth on different solid media markedly affects the properties and behaviors of Opa+ gonococci, p. 771–776. *In* Proceedings of the Eighth International Pathogenic Neisseria Conference.

53. **Swanson, J.** 1973. Studies on gonococcus infection. IV. Pili: their role in attachment of gonococci to tissue culture cells. J. Exp. Med. **137:**571–589.

54. **Theriot, J. A., J. Rosenblatt, D. A. Portnoy, P. J. Goldschmidt-Clermont, and T. J. Mitchison.** 1994. Involvement of profilin in the actin-based motility of *L. monocytogenes* in cells and in cell-free extracts. Cell **76:**505–517.

55. **van Putten, J. P., T. D. Duensing, and J. Carlson.** 1998. Gonococcal invasion of epithelial cells driven by P.IA, a bacterial ion channel with GTP binding properties. J. Exp. Med. **188:**941–952.

56. **van Putten, J. P., T. D. Duensing, and R. L. Cole.** 1998. Entry of OpaA+ gonococci into HEp-2 cells requires concerted action of glycosaminoglycans, fibronectin and integrin receptors. Mol. Microbiol. **29:**369–379.

57. **van Putten, J. P., H. U. Grassme, B. D. Robertson, and E. T. Schwan.** 1995. Function of lipopolysaccharide in the invasion of *Neisseria gonorrhoeae* into human mucosal cells. Prog. Clin. Biol. Res. **392:**49–58.

58. **Vasselon, T., J. Mounier, R. Hellio, and P. J. Sansonetti.** 1992. Movement along actin filaments of the perijunctional area and de novo polymerization of cellular actin are required for *Shigella flexneri* colonization of epithelial Caco-2 cell monolayers. Infect. Immun. **60:**1031–1040.

59. **Virji, M., K. Makepeace, D. J. Ferguson, and S. M. Watt.** 1996. Carcinoembryonic antigens (CD66) on epithelial cells and neutrophils are receptors for Opa proteins of pathogenic *Neisseriae*. Mol. Microbiol. **22:**941–950.

60. **Virji, M., S. M. Watt, S. Barker, K. Makepeace, and R. Doyonnas.** 1996. The N-domain of the human CD66a adhesion molecule is a target for Opa proteins of *Neisseria meningitidis* and *Neisseria gonorrhoeae*. Mol. Microbiol. **22:**929–939.

61. **Waldbeser, L. S., R. S. Ajioka, A. J. Merz, D. Puaoi, L. Lin, M. Thomas, and M. So.** 1994. The opaH locus of *Neisseria gonorrhoeae* MS11A is involved in epithelial cell invasion. Mol. Microbiol. **13:**919–928.

62. **Wang, J., S. D. Gray-Owen, A. Knorre, T. F. Meyer, and C. Dehio.** 1998. Opa binding to cellular CD66 receptors mediates the transcellular traversal of *Neisseria gonorrhoeae* across polarized T84 epithelial cell monolayers. Mol. Microbiol. **30:**657–671.

63. **Weel, G. F. L., C. T. P. Hopman, and J. P. M. Van Putten.** 1991. In situ expression and localization of *Neisseria gonorrhoeae* opacity proteins in infected epithelial cells: apparent role of Opa proteins in cellular invasion. J. Exp. Med. **173:**1395–1405.

64. **Wolfgang, M., P. Lauer, H. S. Park, L. Brossay, J. Hebert, and M. Koomey.** 1998. PilT mutations lead to simultaneous defects in competence for natural transformation and twitching motility in piliated *Neisseria gonorrhoeae*. Mol. Microbiol. **29:**321–330.